Electronic Supplementary Information

Preparation of synergistically reinforced transparent bio-polycarbonate nanocomposites with highly dispersed cellulose nanocrystals

Seul-A Park,[a1] Youngho Eom,[a1] Hyeonyeol Jeon,[a1] Jun Mo Koo,[a] Eun Seong Lee,[b] Jonggeon Jegal,[a] Sung Yeon Hwang,[*ac] Dongyeop X. Oh,[*ac] and Jeyoung Park[*ac]

Experimental section

Materials

Spray-dried cellulose nanocrystals (CNCs) were purchased from the University of Maine (USA). Isosorbide (ISB, 99.8%) was supplied by Roquette Frères (France) and used after recrystallization from acetone. 1,4-Cyclohexanedimethanol (CHDM, 99.5%) with a 74 mol% trans-isomer was supplied by SKC Co. (Korea). Tetramethylammonium hydroxide (TMAH, 97%), diphenyl carbonate (DPC, 99%), triphenylphosphite (TPP, 97%), 2,6-di-tert-butyl-4-hydroxymethylphenol (DBHP, 97%), poly(bisphenol-A carbonate) (average M_w of 45,000 g/mol), chloroform (HPLC grade, 99.8%), dimethylsulfoxide (99.9%), methanol (99.9%), and 1-butanol (99.4%) were purchased from Sigma-Aldrich (USA). All chemicals were used without further purification, unless stated.

In situ polycondensations to obtain nanocomposites (I-series)

The polymerization procedure of poly(ISB-*co*-CHDM carbonate) was described in a previous report.[1] A typical *in situ* polymerization procedure of **ISB-I-0.05** is described below. ISB (29.81 g, 0.204 mol) was heated in an oven at 60 °C under a N_2 atmosphere for 2 h to bring it in a melt state. CNC (25 mg) of 0.05 wt% compared to the target polymer yield of 50 g added into the melted ISB was sonicated for 2 min by using a probe-tip sonicator (VCX750, Sonics

& Materials Inc., USA) under the conditions of 750 W, 20 kHz, 40% power output, and repeating cycles of 3 s purge and 2 s rest. CNC dispersed homogeneously in ISB, CHDM (12.61 g, 0.087 mol), and DPC (62.43 g, 0.291 mol) were added into a 300 ml dried glass vessel. TMAH (100 mg, 0.55 mmol), as a catalyst, and TPP (100 mg, 0.32 mmol) and DBHP (100 mg, 0.42 mmol), as thermostabilizers, were added. The reactor in an oil bath was heated to 150 °C and maintained for 2 h under a nitrogen atmosphere. The temperature was raised to 180 °C under a vacuum of 100 torr for 1 h to distill off phenol (byproduct). Then, the temperature was gradually raised to 240 °C and the pressure was gradually diminished to <0.1 mTorr. The polymerization was terminated after 20−30 min. After the reactor pressure was stabilized to atmospheric pressure by nitrogen purge, the final polymer product (49 g, 98%) was collected and crushed under liquid N_2 for 15 s (WB-01, Sanplatec, Japan, 820 W, 28,000 rpm, repeating cycles of 3 s purge and 2 s rest). M_n 30,700 g/mol, PDI: 1.96. ^{1}H NMR ($CDCl_3$, 300 MHz, ppm): 5.06, 4.86, 4.52, 4.08–3.86, 1.80, 1.63, 1.52, 1.39, 1.01. ^{13}C NMR ($CDCl_3$, 75 MHz, ppm): 155.65-153.42, 86.10, 81.66, 73.42, 70.70, 50.63, 37.14, 34.59, 28.66, 25.18.

Solution blending for nanocomposites (B-series)

A typical solution-blending procedure of **ISB-B-0.05** is described below. The crushed homo-poly(ISB-*co*-CHDM carbonate) (**ISB-0**, 10 g) and CNC (5 mg) were added in chloroform (100 g) and stirred at 25 °C for 1 h. The solution (10 wt%) was sonicated for 10 min using a bath sonicator (SD-D400H, Mujigae Co. Ltd., Korea, 400 W, 60 Hz, 42% of power output). The homogeneous solution (10 wt%) was dried and crushed under liquid N_2 for 10 s.

Preparation of solvent-casting films

In situ type: the crushed polymer (I-series polycarbonates, 1 g) added in chloroform (10 g) was stirred at 25 °C for 1 h. The homogeneous solution (10 wt%) was dried in a glass dish (90 mm in diameter) under ambient conditions for 2 days to obtain ~90-μm-thick films.

Blend type: the crushed B-series polycarbonates (1 g) and external CNC (0.05 to 0.5 wt% compared to polymer) were added in chloroform (10 g) and stirred at 25 °C for 1 h. The solution (10 wt%) was sonicated for 10 min using a bath sonicator. The homogeneous solution (10 wt%) was dried in a glass dish (90 mm in diameter) under ambient conditions for 2 days to obtain ~90-μm-thick films.

Preparation of melt injection-molded specimens

The crushed polycarbonate powder samples were initially dried at 60 °C under vacuum for 24 h. The specimens for the mechanical tests were prepared with a Haake™ Minijet of Thermo Scientific (USA). The temperature of the cylinder, cylinder exposure time, injection pressure, filling time, and mold temperature were 200 °C, 5 min, 500 bar, 15 s, and 150 °C, respectively.

Characterization of *in situ*-polymerized CNC from model study of ISB-I-5 and comparison with ISB-B-5

To investigate the CNC surface modification, excessive CNC (5 wt% per target polymer yield) pre-dispersed in ISB was *in situ*-polymerized to **ISB-I-5**, and CNC (5 wt%) was solution-blended with a homo-polymer in chloroform to prepare **ISB-B-5**. All preparation procedures are identical to those described above. To separate out the used CNC from the polymer part,

homogeneous nanocomposite (50 g) solutions in chloroform (1 L) were centrifuged at 10,000 rpm for 10 min. The supernatant of the likely polycarbonate part was discarded and the submerged powder was obtained. To completely remove the polycarbonate portion, the powder redispersed in the chloroform solution was centrifuged repeatedly 10 times.

The chemical structures of the centrifuged powder, probably used CNC, were identified by Fourier transform-infrared (FT-IR), solid-state cross-polarization/magic-angle-spinning ^{13}C nuclear magnetic resonance (CP/MAS ^{13}C NMR), and field-emission scanning electron microscopy (FE-SEM). FT-IR spectra were collected on an iS50-FT-IR (NICOLET, USA) equipped with an attenuated total reflection mode on a diamond ZnSe crystal. The scanning range was between 4,000 and 650 cm^{-1} at a resolution of 0.4 cm^{-1} and the number of scans was 128. The CP/MAS ^{13}C NMR experiments were conducted on a 400 MHz (9.4 Tesla) Bruker Avance spectrometer (Avance III HD 400, Bruker, USA) using a 4 mm HX-MAS probe. The standard ^{13}C CP experiments were collected under 10 kHz MAS at 298 K. Repetition delays of 3 s and contact time of 2,000 s were used. The number of scans for the accumulation of the solid-state CP/MAS ^{13}C NMR spectra was 2048. The centrifuged powder dispersed in various organic solvents was spin/drop-casted on a pre-washed Si wafer and dried under vacuum for 2 days. The dried morphology was directly observed without any conductive coating applied using FE-SEM (MERLIN, Carl Zeiss NTS, Germany). The images were characterized at a voltage of 0.5−1.0 kV to reduce the charging of samples.

Other characterizations

^{1}H and ^{13}C NMR spectroscopy experiments were conducted using a Bruker Avance 300 MHz spectrometer (USA). $CDCl_3$ with tetramethylsilane was used as a deuterium solvent.

The bio-carbon content of the polymer was measured by accelerator mass spectroscopy (AMS) using a MICADAS 200 kV from IonPlus (Switzerland).

The number-averaged molecular weight (M_n), weight-averaged molecular weight (M_w), and polydispersity index of the polymers relative to linear polystyrene standards were measured using gel permeation chromatography (GPC). The experiments were performed with Acquity APC XT columns at 40 °C (Mixed bed, maximum pore size 450 Å) equipped with an Acquity refractive index detector using chloroform as a mobile phase.

The glass transition temperature (T_g) was measured by differential scanning calorimetry using a Q-2000 (TA instruments, USA). The heating/cooling rate was 10 °C min^{-1} from 30 to 180 °C under a nitrogen atmosphere.

The decomposition temperature was determined using Pyris 1 (Perkin Elmer, USA). The samples were heated from 30 to 800 °C at a heating rate of 10 °C min^{-1} under N_2 flow.

Tensile properties were measured using a universal testing machine (Instron 5943, UK), loaded with a 1 kN load cell and a drawing rate of 10 mm min^{-1} at room temperature of 25 °C. The test specimens had a dumbbell shape, which was 25.5, 3.11, and 3.1 mm in length, width, and thickness, respectively, according to ASTM D638-03.

The impact strength test was measured at room temperature of 25 °C with a pendulum impact testing machine (HIT-2492, Jinjian Testing Instrument, China) in accordance with KS M ISO 180:2012. All impact test samples were V-shape-notched. The standard specimen for ISO is a Type1A multipurpose specimen, having dimensions of 80 × 10 × 4 mm^3.

The rheological measurements for investigating the CNC dispersions in the melted polymer matrix were performed at 200 °C with an Anton Paar MCR 302 rheometer (Anton Paar, Austria)

using a parallel-plate geometry (plate diameter of 25 mm) at a gap of around 1 mm. The complex viscosity (η*), storage modulus (G′), and loss modulus (G″) were measured during a frequency sweep under an angular frequency (ω) range of 0.1 to 100 rad s^{-1} at 200 °C. A logarithmic plot of G′ vs. G″, so-called modified Cole-Cole plot or Han plot, is usually employed for the description of the structural differences of heterogeneous polymeric materials at a fixed temperature. For all samples, the slope of the Cole-Cole plot was obtained in the terminal region using four data points in the initial stage (0.1−0.4 rad s^{-1}) of the curves. In case of absolutely homogeneous polymeric materials, as a rule, the G′ is proportional to the square of the ω ($G' \sim \omega^2$), whereas the G″ increases linearly with the ω ($G'' \sim \omega$). Thus, the deviation of slope from 2 is a measure of the heterogeneity of the system.

The fractured surface morphology of the tensile and impact tested specimens was observed using FE-SEM (Hitach SU-8220, Japan) at an accelerating voltage of 5 kV. The specimens were sputter-coated with a thin platinum alloy to reduce the charge effects, using an Emitech K575X sputtering coater (Emitech, UK), prior to SEM observation.

The X-ray tomography experiments were performed using SkyScan 1176 (Bruker-micro CT, Belgium) to observe the 3D morphology of the nanofillers within the polymer matrix by transmitting the X-rays. The used SkyScan 1176 system had an X-ray source operated at 40 kV/398 μA. The injection-molded nanocomposite was cut into a small piece of dimensions 10 × 10 × 2 mm^3. The 3D images generated by X-ray were recorded with a rotation of 0.3° by rotating the sample 360°. The total acquisition time was approximately 1 h for each sample.

The magnified morphologies of the injection-molded nanocomposite specimens were observed using high-resolution TEM (Bio-TEM, FEI, Tecnai G2 F20, 200 kV, ThermoFisher, USA). The nanocomposite specimens for TEM measurement (70 nm) were prepared by cryo-

microtoming (EM UC7, Leica, Germany), which was transferred onto carbon-coated copper grids (TED Pella Inc., 200 Mesh Copper Grid, Sweden). The sectioned films were stained by 1% osmium tetroxide vapor for 45 min to observe CNC clearly, and then rinsed with deionized water and dried.

***In vivo* bio-compatibility test.**[2]

A public contract clinical research organization, Daegu Gyeongbuk medical innovation foundation (http://www.dgmif.re.kr/eng/index.do), performed all surgical procedures with the approval of the National Institutional Review Board. The samples were implanted in male Sprague–Dawley rats (8-week-old, 250−300 g) (n = 5), which were allowed free access to water and food in a temperature- and humidity-controlled room (22 °C/50%) with a 12/12 h day/night cycle. Each rat was anesthetized with an intramuscular injection of 50 mg ml^{-1} Zoletil 50 (tiletamine and zolazepam; Virbac, France) and 23 mg ml^{-1} Rompun (xylazine; Bayer, Germany), and the scalp was incised carefully. One experimental sample and one negative control (HDPE) film (10 mm diameter) were implanted in two regions (15 mm incision) of a rat's subcutaneous tissues. The incised skin was closed with 4/0 Dafil sutures (Ethicon, USA) and disinfected with a povidone after the procedure. After the surgery, the rats were bred in their cages for 12 weeks, and then, sacrificed for histological analyses.

The tissue samples were routinely dehydrated, paraffin-embedded, cut, and stained with haematoxylin and eosin. Then, their cross-sections were examined and semi-quantitatively evaluated according to the International Standard (ISO 10993-6, Annex A); "criteria for biological evaluation of the local effects of medical devices after implantation" by a pathologist. The local effects were evaluated by comparing the tissue responses caused by the experimental samples and negative control. The scoring system was a histological evaluation

of the extent of the area affected. The presence, number, and distribution of the lymphocytes, polymorphonuclear cells, macrophages, plasma cells, giant cells, and necrosis were evaluated. The tissue changes caused by fatty infiltration, neovascularization, and fibrosis were evaluated.

Table S1. Solubility parameters by Hoftyzer-van Krevelen (HVK).

Name	Solubility parameter by HVK in $(MPa)^{1/2}$			
	δ_d	δ_p	δ_h	δ
Cellulose repeating unit[a]	4.79	5.59	29.93	30.82
Isosorbide[b]	4.45	4.38	22.15	23.01
ISB-carbonate repeating unit[c]	4.64	4.34	13.35	14.78
CHDM-carbonate repeating unit[d]	4.31	2.59	8.68	10.03
BPA-carbonate repeating unit[e]	4.67	2.52	7.57	9.24

[a] Chemical structure and calculation of cellulose repeating unit.

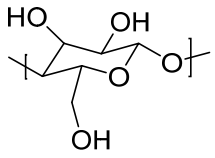

Functional group	No	F(di)	F(pi)	E(hi)	V($cm^3\ mol^{-1}$)
CH_2	1	270	0	0	16.1
		270	0	0	16.1
CH	5	80	0	0	-1
		400	0	0	-5
OH	3	210	500	20000	13
		630	1500	60000	39
ether O	2	100	400	3000	3.8
		200	800	6000	7.6
ring	1	190	0	0	16
		190	0	0	16
Sum		1690	2300	66000	73.7
δ	d	4.79			
	p	5.59			
	h	29.93			
Solubility parameter for HVK		**30.82**			

[b] Chemical structure and calculation of isosorbide.

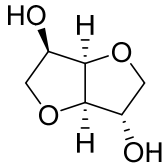

Functional group	No	F(di)	F(pi)	E(hi)	V($cm^3\ mol^{-1}$)
CH_2	2	270	0	0	16.1
		540	0	0	32.2
CH	4	80	0	0	-1
		320	0	0	-4
OH	2	210	500	20000	13
		420	1000	40000	26
O	2	100	400	3000	3.8
		200	800	6000	7.6
ring	2	190	0	0	16
		380	0	0	32
Sum		1860	1800	46000	93.8
δ	d	4.45			
	p	4.38			
	h	22.15			
Solubility parameter for HVK		**23.01**			

[c] Chemical structure and calculation of ISB-carbonate repeating unit.

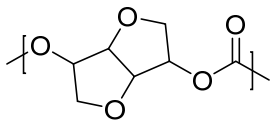

Functional group	No	F(di)	F(pi)	E(hi)	V(cm^3 mol^{-1})		
CH_2	2	270	0	0	16.1		
		540	0	0	32.2		
CH	4	80	0	0	-1		
		320	0	0	-4		
ether O*	3	100	400	3000	3.8		
		300	1200	9000	11.4		
ring	2	190	0	0	16		
		380	0	0	32		
COO	1	390	490	7000	22		
		390	490	7000	22		
Sum		1930	1690	16000	93.6	89.8	Volume correction
δ	d	4.54				4.64	
	p	4.25				4.34	
	h	13.07				13.35	
Solubility parameter for HVK		**14.48**				**14.78**	

[d] Chemical structure and calculation of CHDM-carbonate repeating unit.

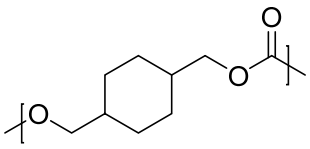

Functional group	No	F(di)	F(pi)	E(hi)	V(cm^3 mol^{-1})		
CH_2	6	270	0	0	16.1		
		1620	0	0	96.6		
CH	2	80	0	0	-1		
		160	0	0	-2		
ether O*	1	100	400	3000	3.8		
		100	400	3000	3.8		
ring	1	190	0	0	16		
		190	0	0	16		
COO	1	390	490	7000	22		
		390	490	7000	22		
Sum		2460	890	10000	136.4	132.6	Volume correction
δ	d	4.25				4.31	
	p	2.55				2.59	
	h	8.56				8.68	
Solubility parameter for HVK		**9.89**				**10.03**	

[e] Chemical structure and calculation of BPA-carbonate repeating unit.

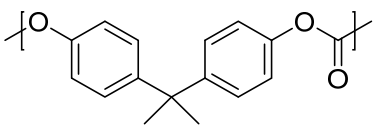

Functional group	No	F(di)	F(pi)	E(hi)	V(cm^3 mol^{-1})		
CH_3	2	420	0	0	33.5		
		840	0	0	67		
>C<	1	-70	0	0	-19.2		
		-70	0	0	-19.2		
ether O*	1	100	400	3000	3.8		
		100	400	3000	3.8		
Bz	2	1270	110	0	52.4		
		2540	220	0	104.8		
COO	1	390	490	7000	22		
		390	490	7000	22		
Sum		3800	1110	10000	178.4	174.6	Volume correction
δ	d	4.62				4.67	
	p	2.49				2.52	
	h	7.49				7.57	
Solubility parameter for HVK		**9.14**				**9.24**	

Table S2. Polymerization information and results.

	Method	M_n[a]	M_w[a] (kg mol^{-1})	PDI[a]	T_g[b] (ºC)	T_{d5}[c] (ºC)	T_{max}[c] (ºC)
ISB-0	Normal polymerization	31	60	2.0	130	383	426
ISB-I-0.05	*In situ* polymerization	37	73	2.0	131	387	425
ISB-I-0.1		35	67	1.9	131	386	422
ISB-I-0.3		31	60	2.0	128	387	425
ISB-I-0.5		20	37	2.0	120	378	424
ISB-I-5		4	7	2.1	92.5	371	427
ISB-B-0.05	Solution blending	31	60	2.0	130	389	428
ISB-B-0.1					126	390	428
ISB-B-0.3					126	383	423
ISB-B-0.5					119	389	428
BPA-0	Sigma	27	46	1.8	150	504	539
BPA-B-0.05	Solution blending				146	486	553
BPA-B-0.1					147	497	560
BPA-B-0.3					146	490	565
BPA-B-0.5					146	513	561

[a] Determined by chloroform-GPC using polystyrene standards (refractive index detector).

[b] Measured by differential scanning calorimetry with a heating rate of 10 °C min^{-1} (second scan).

[c] Degradation temperature for 5% weight loss (T_{d5}) and the maximum degradation rate temperature (T_{max}) were measured by thermogravimetric analysis with a heating rate of 10 °C min^{-1}.

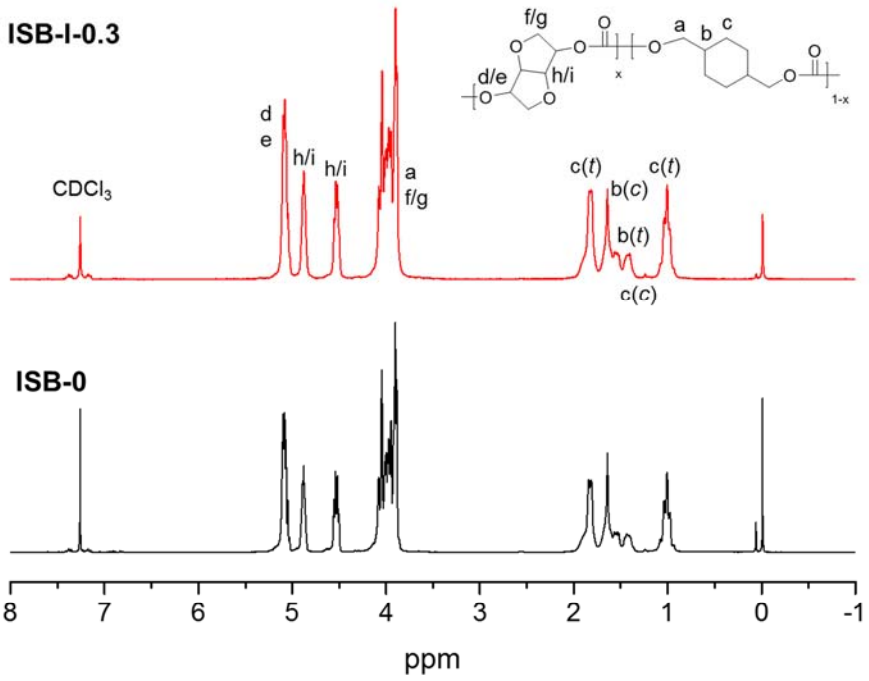

(eq.) Incorporated percentage of ISB (mol%) $= \frac{\int_{4.5}^{5.1} 4H_{ISB}}{\int_{3.8}^{4.2}(4H_{ISB}+4H_{CHDM})} \times 100 = \frac{\int(d+i+f+g)}{\int(a+e+h)} \times 100$

- Incorporated ISB repeating unit (mol%) of **ISB-0** $= \frac{1.000+0.486+0.484}{2.833} \times 100 = 69.5$ mol%

- Weight-based biomass-derived ISB content of **ISB-0** $= \frac{69.5\times144.13}{(69.5\times172.14)+(30.5\times170.21)} \times 100 = 58.4$ wt%

- Incorporated ISB repeating unit (mol%) of **ISB-I-0.3** $= \frac{1.000+0.499+0.508}{2.843} \times 100 = 70.6$ mol%

- Weight-based biomass-derived ISB content of **ISB-I-0.3** $= \frac{70.6\times144.13}{(70.6\times172.14)+(29.4\times170.21)} \times 100 = 59.3$ wt%

Figure S1. ^{1}H NMR spectra and calculation of the incorporated ratio of ISB in mol% and biomass-wt% of **ISB-0** and **ISB-I-0.3**.

- Theoretical biomass carbon content (bio-carbon content) can be calculated by the following equation.

Bio-carbon contents from ISB of **ISB-0**= $\frac{The\ number\ of\ carbon\ atoms\ in\ ISB\ repeating\ unit}{The\ number\ of\ carbon\ atoms\ in\ total\ repeating\ unit} \times 100 = \frac{6\times69.5}{7\times69.5+9\times30.5} \times 100 = 54.8\%$

Bio-carbon contents from ISB of **ISB-I-0.3**= $\frac{The\ number\ of\ carbon\ atoms\ in\ ISB\ repeating\ unit}{The\ number\ of\ carbon\ atoms\ in\ total\ repeating\ unit} \times 100 = \frac{6\times70.6}{7\times70.6+9\times29.4} \times 100 = 55.8\%$

- Experimental bio-carbon content measured by the ratio of ^{14}C to ^{12}C following ASTM D6866B-18 using AMS was determined by the following equations:[3]

$\Delta^{14}C = [(^{14}A_s - ^{14}A_r)/ ^{14}A_r] \times 1000$ (‰, permillage)

$pMC = \Delta^{14}C/10 + 100$ (%, percent)

Bio-carbon content = $pMC \times 100.5$ (%, percent)

($^{14}A_s$ and $^{14}A_r$ are the ratios of ^{14}C and ^{12}C between sample and reference material)

- Bio-carbon content was measured two times and corrected by a factor of 100.5 in 2018 (ASTM D6866-18, Method B, Table 1 & Standard Reference Material (SRM) for oxalic acid 4990C, NIST, USA).

	pMC	**Bio-carbon content (%)**
ISB-0	57.21	57 (±3)
ISB-I-0.3	57.32	57 (±3)

Figure S2. Theoretical calculation and experimental measurement by AMS for ^{14}C-based biomass carbon contents of **ISB-0** and **ISB-I-0.3**.

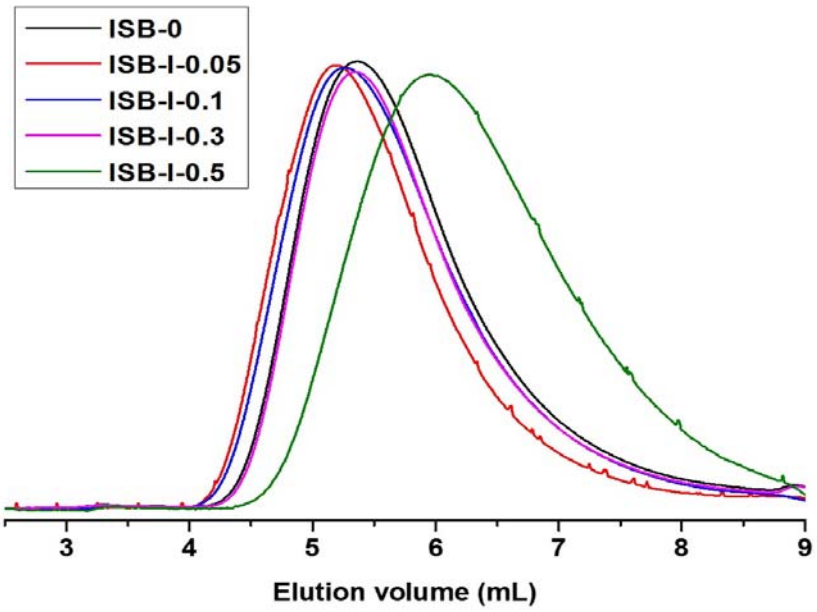

Figure S3. Chloroform-GPC profiles of **ISB-0** and **ISB-I-*N*** series.

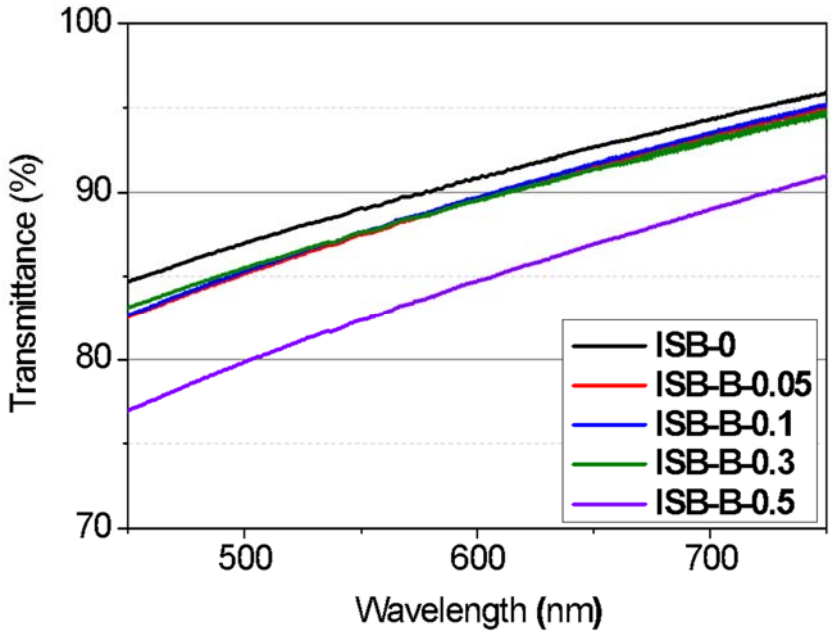

Figure S4. Transmission spectra of solution-casted films of **ISB-B-*N*** series.

Figure S5. Photograph of scaled-up solution-casted polycarbonate film (diameter of 17 cm).

Movie S1. Colorless transparent **ISB-I-0.3** film on the mobile device demonstrating touch screen.

Table S3. Molecular weights of polymer nanocomposites before/after melt processing at 200 ºC.

	Pristine		After melt injection	
	M_w (kg mol^{-1})	PDI	M_w (kg mol^{-1})	PDI
ISB-0	60	2.0	62	1.9
ISB-I-0.3	60	2.0	59	2.0
ISB-B-0.3	60	2.0	59	2.0
BPA-0	46	1.8	46	1.9

*M_w and PDI were d*etermined by chloroform-GPC using polystyrene standards (refractive index detector).

Table S4. Information on tensile properties.

	Young's modulus (GPa)	Ultimate tensile strength (MPa)	Elongation at break (%)	Toughness (MJ m^{-3})	Incremental folds of toughness
ISB-0	2.6 ± 0.05	83 ± 5.8	15 ± 1.1	9.3 ± 0.7	-
ISB-I-0.05	2.1 ± 0.05	81 ± 2.0	30 ± 1.3	18 ± 1.2	1.9
ISB-I-0.1	1.9 ± 0.07	85 ± 0.8	24 ± 1.8	15 ± 1.2	1.6
ISB-I-0.3	1.9 ± 0.07	93 ± 0.8	54 ± 1.5	40 ± 1.1	4.3
ISB-I-0.5	1.8 ± 0.13	59 ± 2.6	4.5 ± 0.1	1.5 ± 0.1	0.16
ISB-B-0.05	2.5 ± 0.03	81 ± 0.9	38 ± 1.7	23 ± 2.9	2.5
ISB-B-0.1	2.3 ± 0.02	79 ± 0.1	50 ± 3.4	31 ± 1.4	3.3
ISB-B-0.3	2.4 ± 0.02	77 ± 0.3	55 ± 2.0	33 ± 3.3	3.5
ISB-B-0.5	2.4 ± 0.02	40 ± 5.5	2 ± 0.7	0.4 ± 0.9	0.04
BPA-0	1.7 ± 0.05	67 ± 2.1	51 ± 3.3	29 ± 1.2	-
BPA-B-0.05	1.8 ± 0.10	69 ± 1.4	51 ± 0.8	28 ± 0.8	0.96
BPA-B-0.1	1.8 ± 0.08	66 ± 0.4	36 ± 1.1	18 ± 0.7	0.63
BPA-B-0.3	1.8 ± 0.04	70 ± 1.0	57 ± 1.8	33 ± 1.4	1.13
BPA-B-0.5	1.8 ± 0.04	69 ± 1.2	56 ± 5.5	31 ± 3.3	1.06

Tensile properties were measured by universal testing machine with a constant drawing rate of 10 mm min^{-1}. Toughness was calculated by integrating the tensile stress-strain curve.

Table S5. Tensile reinforcement performances of polycarbonate composites depending on type and content of fillers.

Filler type[a]	Filler content (wt%)	Polymer type	Pristine UTS (MPa)	UTS of composite (MPa)	UTS increase (fold)	UTS increase per unit filler loading[b] ([fold-1] wt%$^{-1}$)	Pristine ε_b (%)	ε_b of composite (%)	ε_b increase (fold)	ε_b increase per unit filler loading[b] ([fold-1] wt%$^{-1}$)	Ref.
CNC	0.05	ISB-PC	83	81	1.0	–0.48	15	38	2.5	31	This work
	0.3		83	93	1.1	0.40	15	54	3.6	8.7	
	0.3	BPA-PC	67	70	1.0	0.15	51	57	1.1	0.39	
	0.5		~46.2	~48	~1.0	~0.08	~56	~46	~0.8	~ –0.36	4
MWNT	0.375		~69	~71	~1.03	~0.08	~42	~50	~1.2	~0.51	5
	2		59	67	1.1	0.07	>100	80	<0.8	< –0.1	6
	0.5		~60	~56	~0.9	~ –0.13	~90	~80	~0.9	~ –0.22	7
MWNT-*g*	1		60.6	73.9	1.2	0.22	97.4	94.2	1.0	~ –0.03	8
GNP	3		59	~58	~1.0	~0	-	-	-	-	9
MMT	2		60.8	69.7	1.1	0.07	86.3	15.5	0.2	–0.41	10
	1.5		~64	~68	~1.1	~0.04	~135	~125	~0.9	~ –0.05	11
ETPP-MMT	0.5		~46	~52	~1.1	~0.26	~8.5	~7	~0.8	~ –0.35	12
POSS	2.5		52.0	50.9	1.0	0	115.3	115.0	1.0	0	13
Ph-POSS	2.5		56.1	62.0	1.1	0.04	8.4	8.1	1.0	-0.01	14
A300	1		~71	~73	~1.0	~0.03	~63	~67	~1.1	~0.06	15
$CaCO_3$	1		87.2	91.3	1.0	0.05	165.1	63.3	0.4	–0.62	16
AON	0.5		30	~44	~1.5	~0.93	~6	~6	~1	~0	17

[a] MWNT: Multi-walled carbon nanotube, MWNT-*g*: Functionalized multi-walled carbon nanotube prepared by atom-transfer radical polymerization of styrene and acrylonitrile, GNP: Exfoliated graphite nanoplatelet, MMT: Montmorillonite-based organoclay, ETPP-MMT: Ethyl triphenylphosphonium (ETPP) ion included inside the layer spacing of sodium montmorillonite (Na-MMT), POSS: Polyhedral oligomeric silsesquioxane, Ph-POSS: Polyhedral oligomeric silsesquioxane with phenethyl substituents, A300: Hydrophilic fumed silica of 7 nm size, $CaCO_3$: Calcium carbonate nanoparticles with the size of 80 nm, AON: Aluminum oxide nanowhisker with diameter of 2−4 nm and length of 2800 nm.

[b] UTS/$\mathcal{E}_b$ increase per unit filler loading ([fold-1] wt%$^{-1}$) indicates the reinforcement effectiveness of the filler.

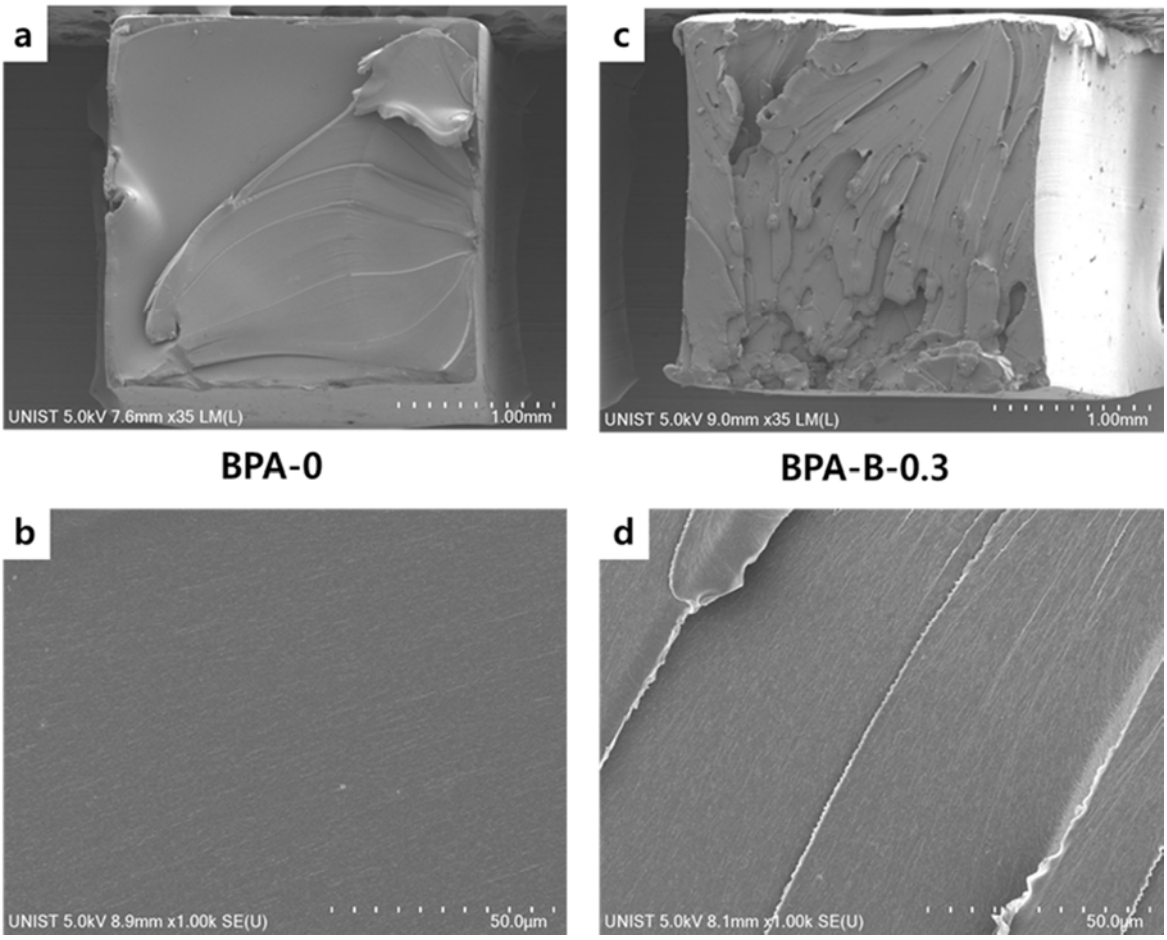

Figure S6. SEM images of fractured surfaces of the tensile-tested specimens ((a,b) **BPA-0**, and (c,d) **BPA-B-0.3**).

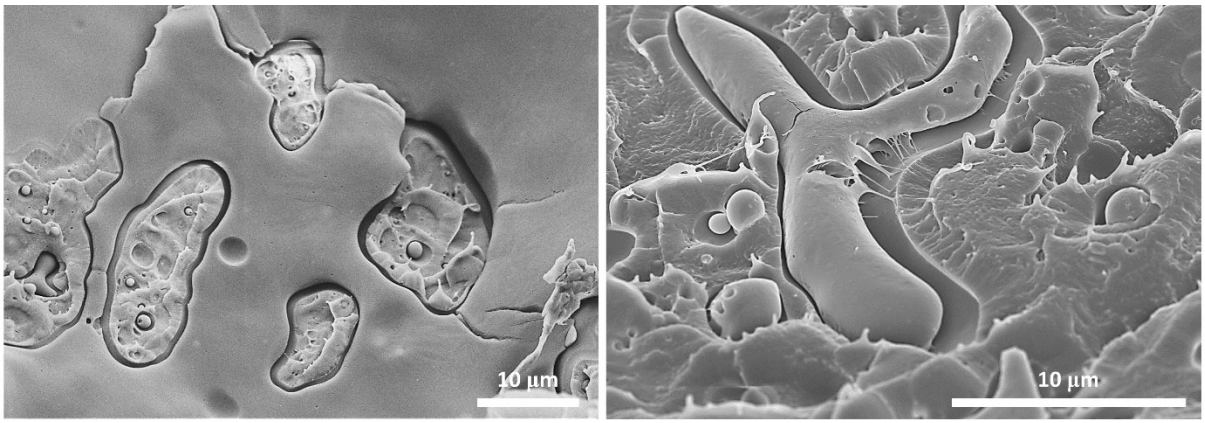

Figure S7. SEM images of micro-sized cavities on the impact-fractured surface of **ISB-I-0.3**.

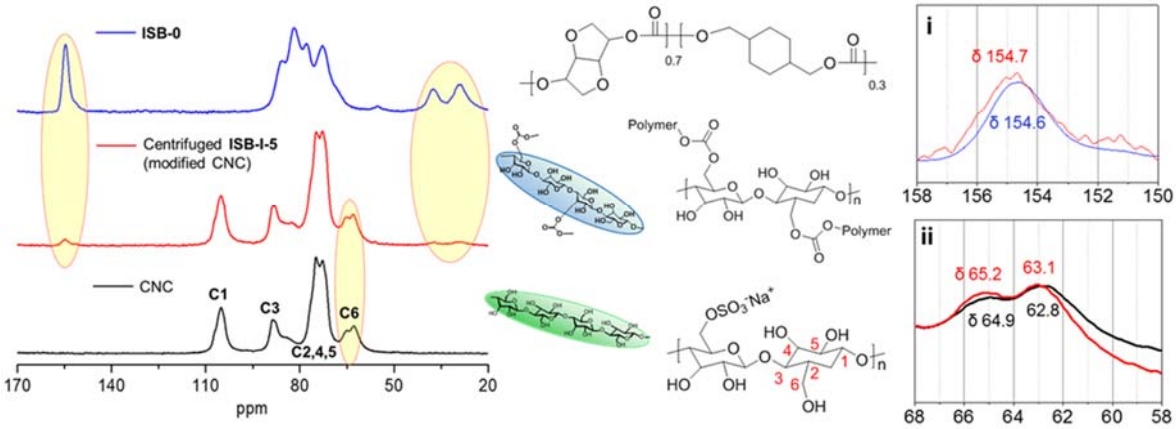

Figure S8. ^{13}C CP/MAS NMR spectra of solid CNC, **ISB-0**, and centrifuged **ISB-I-5** (i: magnified spectra of **ISB-0** and centrifuged **ISB-I-5**, ii: magnified spectra of centrifuged **ISB-I-5** and solid CNC).

- Solid ^{13}C NMR spectrum of centrifuged **ISB-I-5** (modified CNC) indicates two points:

1) Little trace of homo-polymers remained because the shape of the peaks much resembled the spectrum of an untreated CNC solid and 2) the hydroxyl surface of CNC was chemically modified because the carbonyl carbon peak at 154.7 ppm appeared and the adjacent carbon peaks were shifted from the primary alcohol (C6) of CNC to the methylene carbonate group. More specifically, two peaks-top of C6 at 64.9 and 62.8 ppm down-field-shifted to 65.2 and 63.1 ppm, and the proportion of the peak at high ppm increased by transesterification, which de-shields the C6 carbon because of electron-withdrawing carbonate linkage.

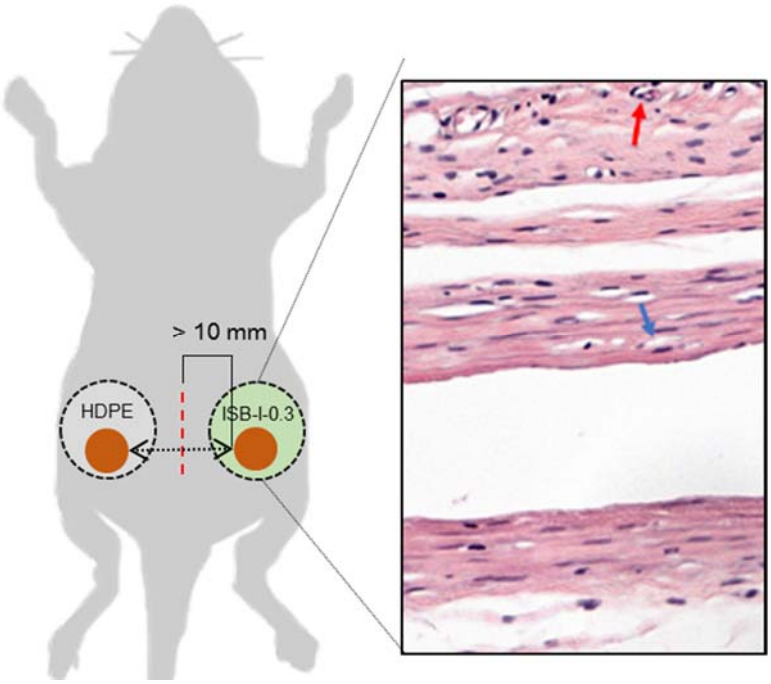

Figure S9. *In vivo* experimental illustration during biocompatibility testing. HDPE, as a negative control, and **ISB-I-0.3** films were implanted into the subcutaneous connective tissue of a rat. Histopathologic tissue images taken 12 weeks after implantation. Arrows indicate inflammatory cells (red: polymorphonuclear cell, blue: macrophage).

- To expand the applications of bio-polycarbonate into biomedical hard devices, including artificial bone and dental brackets, its biocompatibility should be proved. An *in vivo* test was conducted by a contracted clinical research organization by using a rat subcutaneous model following ISO 10993-6 tests for local effects of biomedical devices after implantation. Films (diameter of 1 cm) of **ISB-I-0.3** and high-density polyethylene (HDPE), as a negative control, were implanted into the subcutaneous connective tissue of each rat. The rats were sacrificed 12 weeks after implantation. The histopathologic analyses of the subcutaneous tissues after routine fixing and dyeing processes indicated that **ISB-I-0.3** had acceptable low contents of

inflammatory cells. The degree of inflammatory responses was semi-quantitatively scored by a pathologist in the order of non-irritant < slight < moderate < severe. The **ISB-I-0.3** film achieved a lower inflammatory intensity of "slight," which is an acceptable level for a body-implanted device in the guideline. The results support the potential of **ISB-I-0.3** as a biomedical material.

Supplementary References

1. S.-A. Park, J. Choi, S. Ju, J. Jegal, K. M. Lee, S. Y. Hwang, D. X. Oh and J. Park, *Polymer*, 2017, **116**, 153-159.
2. S.-A. Park, H. Jeon, H. Kim, S.-H. Shin, S. Choy, D. S. Hwang, J. M. Koo, J. Jegal, S. Y. Hwang, J. Park and D. X. Oh, *Nat. Commun.*, 2019, **10**, 2601.
3. ASTM International, ASTM D6866-18 Method B: Standard Test Methods for Determining the Biobased content of Solid, Liquid and Gaseous Samples Using Radiocarbon Analysis. https://www.astm.org/Standards/D6866.htm
4. W. Xu, Z. Qin, H. Yu, Y. Liu, N. Liu, Z. Zhou and L. Chen, *J. Nanopart. Res.*, 2013, **15**, 1562.
5. F. Y. Castillo, R. Socher, B. Krause, R. Headrick, B. P. Grady, R. Prada-Silvy and P. Pötschke, *Polymer*, 2011, **52**, 3835-3845.
6. A. Eitan, F. T. Fisher, R. Andrews, L. C. Brinson and L. S. Schadler, *Compos. Sci. Technol.*, 2006, **66**, 1162-1173.
7. S. Abbasi, P. J. Carreau and A. Derdouri, *Polymer*, 2010, **51**, 922-935.
8. W. S. Choi and S. H. Ryu, *Colloids Surfaces A*, 2011, **375**, 55-60.
9. J. A. King, M. D. Via, F. A. Morrison, K. R. Wiese, E. A. Beach, M. J. Cieslinski and G. R. Bogucki, *J. Compos. Mater.*, 2012, **46**, 1029-1039.
10. J. Feng, J. Hao, J. Du and R. Yang, *Polym. Degrad. Stabil.*, 2012, **97**, 108-117.
11. A. J. Hsieh, P. Moy, F. L. Beyer, P. Madison, E. Napadensky, J. Ren and R. Krishnamoorti, *Polym. Eng. Sci.*, 2004, **44**, 825-837.
12. S. Suin, N. K. Shrivastava, S. Maiti and B. B. Khatua, *Eur. Polym. J.*, 2013, **49**, 49-60.

13. Y. Zhao and D. A. Schiraldi, *Polymer*, 2005, **46**, 11640-11647.
14. M. Sánchez-Soto, D. A. Schiraldi and S. Illescas, *Eur. Polym. J.*, 2009, **45**, 341-352.
15. A. Christmann, P. Ienny, J. C. Quantin, A. S. Caro-Bretelle and J. M. Lopez-Cuesta, *Polymer*, 2011, **52**, 4033-4044.
16. Z. Wang, G. Xie, X. Wang, G. Li and Z. Zhang, *Mater. Lett.*, 2006, **60**, 1035-1038.
17. H. R. Hakimelahi, L. Hu, B. B. Rupp and M. R. Coleman, *Polymer*, 2010, **51**, 2494-2502.